Paweł Stąpór[1]

An enhanced XFEM for the discontinuous Poisson problem

In the paper, the extended finite element method (XFEM) is combined with a recovery procedure in the analysis of the discontinuous Poisson problem. The model considers the weak as well as the strong discontinuity. Computationally efficient low-order finite elements provided good convergence are used. The combination of the XFEM with a recovery procedure allows for optimal convergence rates in the gradient i.e. as the same order as the primary solution. The discontinuity is modelled independently of the finite element mesh using a step-enrichment and level set approach. The results show improved gradient prediction locally for the interface element and globally for the entire domain.

1. Introduction

The aim of the paper is to reach enhanced gradient predictions, as part of the solution of the Poisson equation which represents the mathematical model of a problem. This aim can be achieved with specific enrichment functions as it is shown in [1], however the stability of solution as well as computational cost is then deteriorated. The alternative approach is based on post-processing techniques which do not influence the size of the problem and stability of the solution. During the last decades, a great deal of effort was put in exploring stress improvement procedures for solids and structures and to establish solution error estimates, [2, 3]. Recently, an effective technique has been proposed in [4]. In the case of discontinuous problems, the XFEM approximation can recover the discontinuity of the solution locally using enriched approximation, [5]. The XFEM solution introduce

---

✉ Paweł Stąpór, e-mail: stapor@tu.kielce.pl

[1]Faculty of Management and Computer Modelling, Kielce University of Technology, Kielce, Poland.

the discontinuity through nodal enrichment function, and controls it by additional degrees of freedom. This allows to make the finite element mesh independent of discontinuity location.

If an effective procedure to improve the solution is established, a coarse mesh with low-order elements can be used in the finite element analysis. In the study, we assess the effectiveness of the proposed approach using L_2 and energy norms. The stability of the solution is investigated using the condition number of the underling stiffness matrix.

2. Governing equations

Let us consider a domain Ω with boundary Γ divided into the sub-domains Ω_S and Ω_L, (Fig. 1). The sub-domains are separated from each other by the interface Γ_I. The boundary Γ is composed of the sets Γ_D and Γ_N such that $\Gamma = \Gamma_D \cup \Gamma_N$ and $\Gamma_D \cap \Gamma_N = \emptyset$. The normal vector $\mathbf{n}$ on the external boundary Γ and the outward normal vector $\mathbf{n}_I$, on the interface Γ_I are defined. The evaluation of function $u(\mathbf{x})$ in Ω is governed by the Poisson equation

$$\nabla \mathbf{q}(\mathbf{x}) + f(\mathbf{x}) = 0 \quad \text{in} \quad \Omega, \tag{1}$$

where

$$\mathbf{q}(\mathbf{x}) = -k(\mathbf{x})\nabla^T u(\mathbf{x}) \tag{2}$$

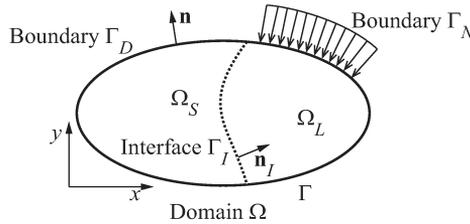and k is the material coefficient, and f denotes a source term.

Fig. 1. Domain Ω split into Ω_L and Ω_S by the interface Γ_I

The essential

$$u(\mathbf{x}) = u_D(\mathbf{x}) \quad \text{at} \quad \Gamma_D \tag{3}$$

and natural

$$-k(\mathbf{x})\nabla u(\mathbf{x}) \cdot \mathbf{n} = q_S(\mathbf{x}) \quad \text{at} \quad \Gamma_N \tag{4}$$

boundary conditions are defined at Γ_D and Γ_N, respectively.

It is assumed that the coefficient k and the function f are discontinuous across the interface boundary Γ_I, which can be written as follows

$$k(\mathbf{x}) = \begin{cases} k_L(\mathbf{x}) & \text{in} \quad \Omega_L, \\ k_S(\mathbf{x}) & \text{in} \quad \Omega_S, \end{cases} \tag{5}$$

$$f(\mathbf{x}) = \begin{cases} f_L(\mathbf{x}) & \text{in} \quad \Omega_L, \\ f_S(\mathbf{x}) & \text{in} \quad \Omega_S. \end{cases} \tag{6}$$

The interface conditions define the jump of the solution and its normal gradient at the boundary Γ_I

$$[[u(\mathbf{x})]] = \alpha(\mathbf{x}) \quad \text{at} \quad \Gamma_I, \tag{7}$$

$$[[-k(\mathbf{x})\nabla u(\mathbf{x}) \cdot \mathbf{n}]] = \beta(\mathbf{x}) \quad \text{at} \quad \Gamma_I. \tag{8}$$

The equivalent form of the problem is derived by multiplying equation (1) by a test function $v(\mathbf{x})$ and integrating separately in each domain. As a result, we obtain the following weak form

$$\int_\Omega \nabla v(\mathbf{x})\mathbf{q}(\mathbf{x})\mathrm{d}\mathbf{x} + \int_\Omega v(\mathbf{x})f(\mathbf{x})\mathrm{d}\mathbf{x} - \int_{\Gamma_N} v(\mathbf{x})q_S(\mathbf{x})\mathrm{d}s + \int_{\Gamma_I} v(\mathbf{x})\beta(\mathbf{x})\mathrm{d}s = 0, \tag{9}$$

with essential (3) and interface (7) conditions.

In order to enforce the interface condition (7) the Lagrange multipliers or penalty methods can be applied what adds the following terms to the equation (9)

1) Lagrange method

$$\int_{\Gamma_I} [[v(\mathbf{x})]]\lambda(\mathbf{x})\mathrm{d}s + \int_{\Gamma_I} v_\lambda(\mathbf{x})([[u(\mathbf{x})]] - \alpha(\mathbf{x}))\mathrm{d}s; \tag{10}$$

2) Penalty method

$$p \int_{\Gamma_I} [[v(\mathbf{x})]][[u(\mathbf{x})]]\mathrm{d}s + p \int_{\Gamma_I} [[v(\mathbf{x})]\alpha(\mathbf{x})\mathrm{d}s, \tag{11}$$

where λ and p are Lagrange multiplier and penalty parameter, respectively.

The finite element formulation of equation (9) for an element e with interface conditions applied using penalty method gives

$$\int_{\Omega_h} \nabla v_h^{(e)}(\mathbf{x})\mathbf{q}_h^{(e)}(\mathbf{x})\mathrm{d}\mathbf{x} + p \int_{\Gamma_I} \left[\left[v_h^{(e)}(\mathbf{x})\right]\right]\left[\left[u_h^{(e)}(\mathbf{x})\right]\right]\mathrm{d}s + \int_{\Gamma_I} v_h^{(e)}(\mathbf{x})\beta(\mathbf{x})\mathrm{d}s$$

$$+ \int_{\Omega_h} v_h^{(e)}(\mathbf{x})f(\mathbf{x})\mathrm{d}\mathbf{x} + p \int_{\Gamma_I} [[v(\mathbf{x})]\alpha(\mathbf{x})\mathrm{d}s - \int_{\Gamma_N} v_h^{(e)}(\mathbf{x})q_S(\mathbf{x})\mathrm{d}s = 0. \tag{12}$$

After the basis functions are introduced, equation (12) can be written in the matrix form

$$\mathbf{K}^{(e)}\mathbf{u}^{(e)} + \mathbf{f}^{(e)} - \mathbf{q}_S^{(e)} = \mathbf{0}, \tag{13}$$

where $\mathbf{u}^{(e)}$ is a vector of nodal unknowns, and $\mathbf{K}^{(e)}$, $\mathbf{f}^{(e)}$ and $\mathbf{q}_S^{(e)}$ are the equivalents of stiffness matrix, load vector and externally applied load, respectively. Their global counterparts are computed through the usual assembly procedure.

3. XFEM

The finite element method uses continuous approximation within individual element. Thus, it can only be applied to solve the discontinuous problems by aligning the mesh with discontinuity. The XFEM is suitable for describing discontinuities in the solution fields independent of the finite element mesh. It is essential, however, to locally apply special approximation functions. The enrichment area is contained to the vicinity of a discontinuity; as a result, the size of the problem remains relatively unchanged.

A solution characteristic of the problem is introduced by adding the enrichment term $u(\mathbf{x}, \mathbf{x}_I)_E$ to the standard finite element approximation $u(\mathbf{x})_C$

$$u_h(\mathbf{x}) = u(\mathbf{x})_C + u(\mathbf{x}, \mathbf{x}_I)_E, \tag{14}$$

where

$$u(\mathbf{x})_C = \sum_{j \in I} N_j(\mathbf{x}) u_j. \tag{15}$$

The enrichment term $u(\mathbf{x}, \mathbf{x}_I)_E$ combines the enrichment functions $\Psi^\alpha(\mathbf{x}, \mathbf{x}_I)$ with a partition of unity (PU) functions $\mathbf{N}(\mathbf{x})$ (usually element shape functions)

$$u(\mathbf{x}, \mathbf{x}_I)_E = \sum_{j \in J} \sum_{\alpha=1}^{m} N_j(\mathbf{x}) \Psi^\alpha(\mathbf{x}, \mathbf{x}_I) a_j^\alpha, \tag{16}$$

where J is the set of nodes enriched by $\Psi^\alpha(\mathbf{x}, \mathbf{x}_I)$, a_j^α are the additional degrees of freedom, I is the set of all nodes and m is the number of enrichment functions and $\mathbf{x}_I$ denotes that a term depends on the interface position.

The finite elements with discontinuous approximation are enriched using the common step-enrichment with shifted-basis, e.g. [6]

$$\begin{aligned} \Psi_j(\mathbf{x}) &= H(\mathbf{x}) - H(\mathbf{x}_j), \\ H(\mathbf{x}) &= \text{sign}(\phi(\mathbf{x})), \end{aligned} \tag{17}$$

where $\phi(\mathbf{x})$ is the level set function (distance function).

Then, the equation (13) is used to obtain unknown coefficients of approximation. Finally, *directly calculated gradient* $\mathbf{q}_h^{(e)}(\mathbf{x})$ in an element is obtained using approximation (14)–(16) and equation (2).

4. Recovery procedure

The solution within each element is represented by equations (15) for non-enriched and (14) for enriched elements. With this assumptions, the quantity $\mathbf{q}_h^{(e)}(\mathbf{x})$ follows from equation (2). We refer to this as the *directly calculated*.

It is well known that, for the low order elements (2-node element in 1D, 3-node element in 2D, etc.) the quality of *directly calculated gradient* is poor as compared to the calculated primary field. In order to improve the convergence and quality, the recovery procedure proposed by Payen and Bathe (2012), [4] is applied to *both non-enriched and enriched elements*.

In the presented formulation, the accurate prediction of the gradient is obtained using a mixed interpolation approach. In this approach, the Lagrange multiplier technique is utilised in order to apply physical relationship (2) over the element volumes. The additional solution variable are then the derivative coefficients $\mathbf{q}^{(e)}$ and Lagrange multipliers $\boldsymbol{\lambda}^{(e)}$, which are defined by internal degrees of freedom. They are related only to the considered element e.

An important feature of the formulation is that the primary problem (12) is decoupled from the calculation of the *enhanced gradient* $\mathbf{q}^{(e)}(\mathbf{x})$.

In the method, the solution is enhanced with

$$\int_{\Omega_h} \delta\xi^{(e)}(\mathbf{x}) \left(\nabla\mathbf{q}^{(e)}(\mathbf{x}) + f(\mathbf{x})\right) d\mathbf{x} = 0 \tag{18}$$

and

$$\int_{\Omega_h} \delta\lambda^{(e)}(\mathbf{x}) \left(\mathbf{q}^{(e)}(\mathbf{x}) + k^{(e)}(\mathbf{x})\nabla u_h^{(e)}(\mathbf{x})\right) d\mathbf{x} = 0. \tag{19}$$

The equation (18) enforces the equilibrium condition for the enhanced gradient, whereas equation (19) represents the projection of the difference in enhanced and directly calculated gradients. Equations (18) and (19) are the basic equations used in the presented procedure.

In general analysis, the standard problem (13) is first solved for $u_h^{(e)}(\mathbf{x})$, then $\mathbf{q}^{(e)}(\mathbf{x})$ is obtained from $u_h^{(e)}(\mathbf{x})$ by applying equations (18) and (19) either to each element e or to a set of elements in the calculation domain.

The proper choice of the interpolating function for $\xi^{(e)}(\mathbf{x})$ and $\lambda^{(e)}(\mathbf{x})$ is the key to ensure a well-posed problem as well as the convergence in the optimal order. In order to deliver improved prediction, a richer space for $\mathbf{q}^{(e)}(\mathbf{x})$ must be assumed than that assumed for $\mathbf{q}_h^{(e)}(\mathbf{x})$. The interpolating functions used in the calculation are those proposed in [4] adopted to the considered problem

$$\begin{aligned}
\mathbf{q}^{(e)}(\mathbf{x}) &= \mathbf{E}_q^{(e)}(\mathbf{x})\bar{\mathbf{q}}^{(e)}, \\
\delta\lambda^{(e)}(\mathbf{x}) &= \mathbf{E}_\lambda^{(e)}(\mathbf{x})\bar{\lambda}^{(e)}, \\
\delta\xi^{(e)}(\mathbf{x}) &= \mathbf{E}_\xi^{(e)}(\mathbf{x})\bar{\xi}^{(e)},
\end{aligned} \tag{20}$$

where the approximation for 1D problems is defined

$$\begin{aligned}
\mathbf{E}_q^{(e)}(\mathbf{x}) &= [1 \quad x \quad x^2], \\
\mathbf{E}_\lambda^{(e)}(\mathbf{x}) &= [1], \\
\mathbf{E}_\xi^{(e)}(\mathbf{x}) &= [1 \quad x]
\end{aligned} \tag{21}$$

and for 2D problems

$$
\mathbf{E}_q^{(e)}(\mathbf{x}) = \begin{bmatrix} 1 & x & y & xy & x^2 & y^2 & 0 & 0 & 0 & 0 & 0 & 0 \\ 0 & 0 & 0 & 0 & 0 & 0 & 1 & x & y & xy & x^2 & y^2 \end{bmatrix},
$$

$$
\mathbf{E}_\lambda^{(e)}(\mathbf{x}) = \begin{bmatrix} 1 & 0 & x & y & 2xy & 0 & 0 & y^2 & x^2 \\ 0 & 1 & -y & 0 & -y^2 & -x & -x^2 & 0 & -2xy \end{bmatrix}, \tag{22}
$$

$$
\mathbf{E}_\xi^{(e)}(\mathbf{x}) = \begin{bmatrix} 1 & x & xy \end{bmatrix}.
$$

Inserting the approximation into equations (18) and (19) one obtains the following system

$$
\begin{bmatrix} \displaystyle\int_\Omega \mathbf{E}_\xi^T(\mathbf{x}) \nabla \mathbf{E}_q(\mathbf{x}) \mathrm{d}\Omega \\ \displaystyle\int_\Omega \mathbf{E}_\lambda^T(\mathbf{x}) \mathbf{E}_q(\mathbf{x}) \mathrm{d}\Omega \end{bmatrix} \mathbf{q} = \begin{bmatrix} \displaystyle\int_\Omega -\mathbf{E}_\xi^T(\mathbf{x}) f(\mathbf{x}) \mathrm{d}\Omega \\ \displaystyle\int_\Omega \mathbf{E}_\lambda^T(\mathbf{x}) k(\mathbf{x}) \nabla^T u_h(\mathbf{x}) \mathrm{d}\Omega \end{bmatrix}. \tag{23}
$$

The elements cut by the interface need a special treatment. Since the solution is discontinues, the area of calculation must be split according to the interface. In this way, two separate equations are solved for such elements.

5. 1D solution – weak discontinuity

In order to test the procedure, 1D problem in $\Omega = \langle 0, 1 \rangle$ is considered. The boundary Γ_I is defined by a single point $x_I = 0.6667$. The Poisson equation (1) has the following terms

$$
k = \begin{cases} k_L = 0.1 & \text{for} \quad \phi(x) < 0, \\ k_S = 1 & \text{for} \quad \phi(x) > 0, \end{cases} \tag{24}
$$

where $\phi(x) = x - x_I$. The homogeneous Dirichlet boundary conditions and interface conditions are introduced

$$
u(0) = u(1) = 0,
$$

$$
[[u(x_I)]] = \left[\left[-k(x_I) \frac{\mathrm{d}u(x_I)}{\mathrm{d}x} \right]\right] = 0, \tag{25}
$$

what means we solve weakly discontinuous problem.

The forcing term is assumed to be a smooth function in the form

$$
f(x) = 10 \sin\left(\frac{2\pi x}{x_I}\right). \tag{26}
$$

The low order finite element is used with standard C^0 continuity shape functions of the form

$$\mathbf{N}^{(e)}(x) = \left[1 - \frac{x}{l} \quad \frac{x}{l}\right],\tag{27}$$

where l is the length of an element and $x \in [0, l]$ represents its local coordinate.

In the recovery procedure an element based approach is adopted. The quadratic approximation for the derivative is assumed. Thus, the approximation of $q^{(e)}(x)$ is expressed by

$$q^{(e)}(x) = \left[1 \quad x \quad x^2\right] \mathbf{q}^{(e)},\tag{28}$$

where $\mathbf{q}^{(e)}$ denotes coefficients of approximation of the enhanced solution for an element e.

For enriched element the enhanced solution contains two functions

$$q^{(e)}(x) = \begin{cases} \left[1 \quad x \quad x^2\right] \mathbf{q}_L^{(e)} & \text{for} \quad \phi(x) < 0, \\ \left[1 \quad x \quad x^2\right] \mathbf{q}_S^{(e)} & \text{for} \quad \phi(x) > 0. \end{cases}\tag{29}$$

Fig. 2a and Fig. 3 show the convergence curves for the 1D problem measured in the H^1 norm

$$H^1 = \|q_{exact} - q\| = \sqrt{\int_\Omega (q_{exact} - q)^2 \mathrm{d}\Omega}.\tag{30}$$

Local and global error norms indicate significant improvement in convergence from $O(h^1)$ to $O(h^3)$ order when the recovery procedure is applied.
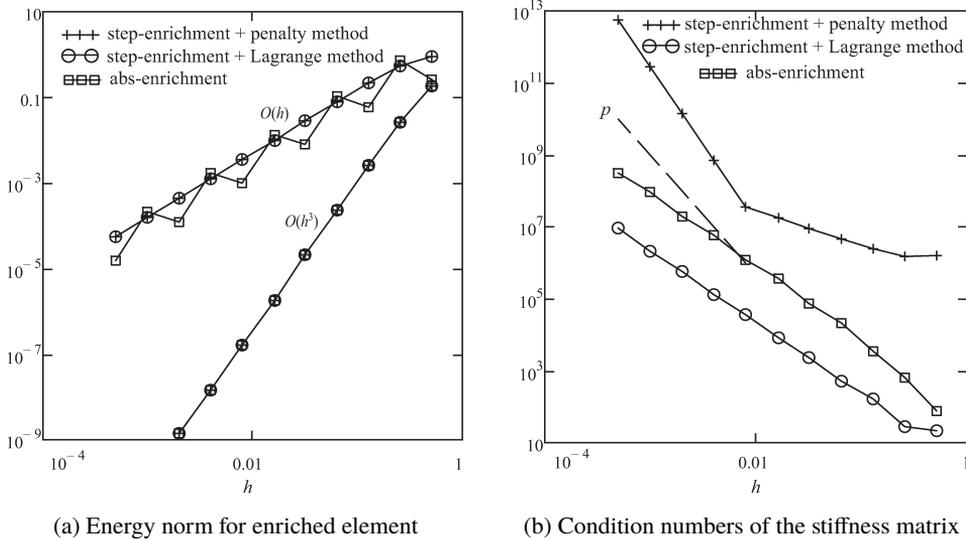

(a) Energy norm for enriched element   (b) Condition numbers of the stiffness matrix

Fig. 2. 1D weak discontinuity problem

The condition number of the underling stiffness matrix is computed according to the L_2 norm. The norm is defined as the maximum of the square root of the column sum-of-squares

$$\|\mathbf{K}\| = \max\left(\sqrt{\sum_{i=1}^{n}(K_{i,j})^2}\right). \tag{31}$$

The condition number of the stiffness matrix is defined as [7]

$$\kappa(\mathbf{K}) = \|\mathbf{K}\|\|\mathbf{K}^{-1}\|. \tag{32}$$

Fig. 2b shows the condition numbers of the stiffness matrix for the considered methods. As can be seen, the condition number of the system is lowest for the Lagrange multiplier method.
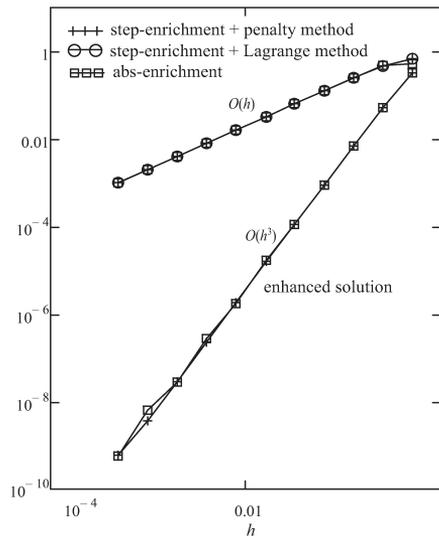
Fig. 3. Energy norm for entire domain

6. 1D solution – strong discontinuity

Now we solve the problem, where the solution as well as its normal gradient are discontinuous across the interface. The analytical solution and coefficient k are given

$$u(x) = \begin{cases} u_L(x) = \sin(\omega x) & \text{for} \quad \phi(x) < 0, \\ u_S(x) = \cos(\omega x) & \text{for} \quad \phi(x) > 0, \end{cases} \tag{33}$$

$$k(x) = \begin{cases} k_L(x) = 0.5 & \text{for} \quad \phi(x) < 0, \\ k_S(x) = 1 & \text{for} \quad \phi(x) > 0, \end{cases} \tag{34}$$

where $\phi(x) = x - x_I$, $x_I = 0.6667$ and $\omega = 10$.

The source term f, Dirichlet and interface boundary conditions follows from analytical solution (33)

$$f(x) = \begin{cases} f_L(x) = -k_L(x)\omega^2 \sin(\omega x) & \text{for} \quad \phi(x) < 0, \\ f_S(x) = -k_S(x)\omega^2 \cos(\omega x) & \text{for} \quad \phi(x) > 0, \end{cases} \tag{35}$$

$$\begin{aligned} u(0) &= 0, \\ u(1) &= \cos(\omega), \\ [[u(x_I)]] &= \sin(\omega x_I) - \cos(\omega x_I), \\ \left[\left[-k(x_I)\frac{\mathrm{d}u(x_I)}{\mathrm{d}x}\right]\right] &= k_L(x_I)\omega\cos(\omega x_I) + k_S(x_I)\omega\sin(\omega x_I). \end{aligned} \tag{36}$$

Fig. 4a shows convergence in enhanced gradient and Fig. 4b presents the condition number of the stiffness matrix. The penalty parameter p was adjusted in a way to achieve the same level of accuracy as for Lagrange method. As for the weak discontinuity problem, the convergence in enhanced gradient reaches $O(h^3)$ order.

(a) Energy norm for enriched element   (b) Condition numbers of the stiffness matrix
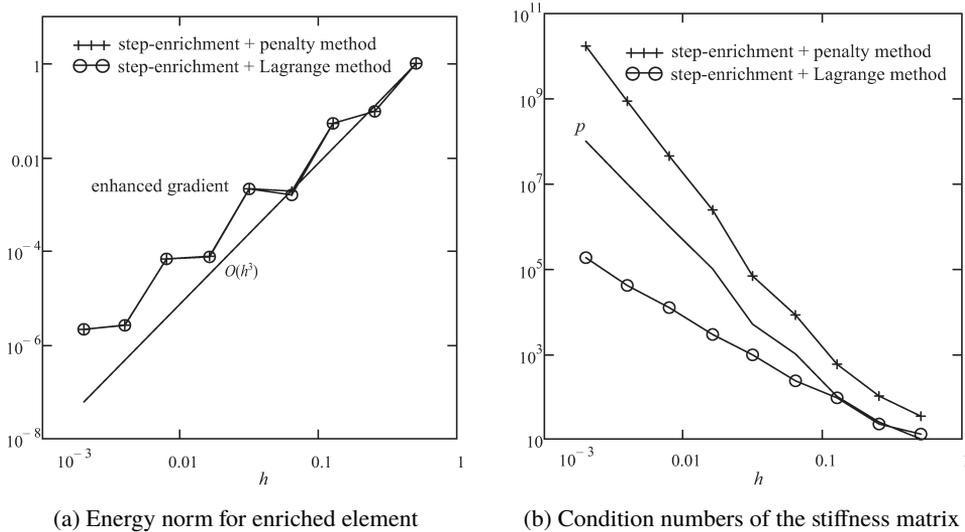
Fig. 4. 1D strong discontinuity

7. 2D solution – strong discontinuity

First we test the procedure for the 2D problem with straight interface. The 1D problem with strong discontinuity was extended to two dimensions, leaving all parameters the same, as well as boundary and interface conditions. For 2D problems, only penalty method was applied. In this case, we observe second-order

convergence for L_2 norm, first order for directly calculated gradient in H^1 norm and $O(h^3)$ order for enhanced gradient, Fig. 5a. Fig. 5b shows the condition number of stiffness matrix for constant value of penalty parameter.
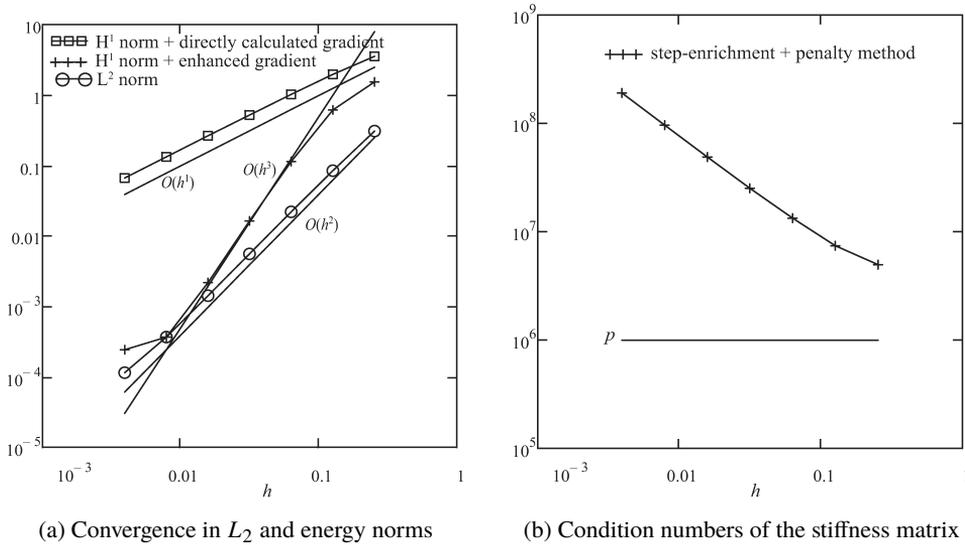

(a) Convergence in L_2 and energy norms

(b) Condition numbers of the stiffness matrix

Fig. 5. 2D straight interface problem

In the second example 2D interface problem with curved interface is considered, [8], the solution u, the coefficients k are given as follows

$$u(\mathbf{x}) = \begin{cases} u_L(\mathbf{x}) = \sin(x + y) & \text{for} \quad \phi(\mathbf{x}) < 0, \\ u_S(\mathbf{x}) = \ln(x^2 + y^2) & \text{for} \quad \phi(\mathbf{x}) > 0, \end{cases} \tag{37}$$

$$k(\mathbf{x}) = \begin{cases} k_L(\mathbf{x}) = \cos(x + y) + 2 & \text{for} \quad \phi(\mathbf{x}) < 0, \\ k_S(\mathbf{x}) = \sin(x + y) + 2 & \text{for} \quad \phi(\mathbf{x}) > 0, \end{cases} \tag{38}$$

where the level set function $\phi(\mathbf{x}) = x^2 + y^2 - 0.25$ represents a circle with radius $R = 0.5$. The Dirichlet and interface boundary conditions, as well as the source function f, follow from the equations (37) and (38). We consider the solution in a square $-1 < x < 1$ and $-1 < y < 1$. The exact solution and its normal gradient are presented in Figs 6a and 6b. The exact gradient in x and y directions are shown in Figs 7a and 7b, respectively.

Figs 8 and 9 show the difference between enhanced and directly calculated gradient for x and y direction and for the mesh size $h = 0.1$.

Fig. 10a shows the energy norm and L_2 norm calculated for the entire domain. In this case, the $O(h^2)$ order for the enhanced solution is not preserved, however, the $O(h^{1.5})$ order is reached. The similar convergence order in energy norm is reported in [8]. Fig. 10b shows the condition number of the stiffness matrix.
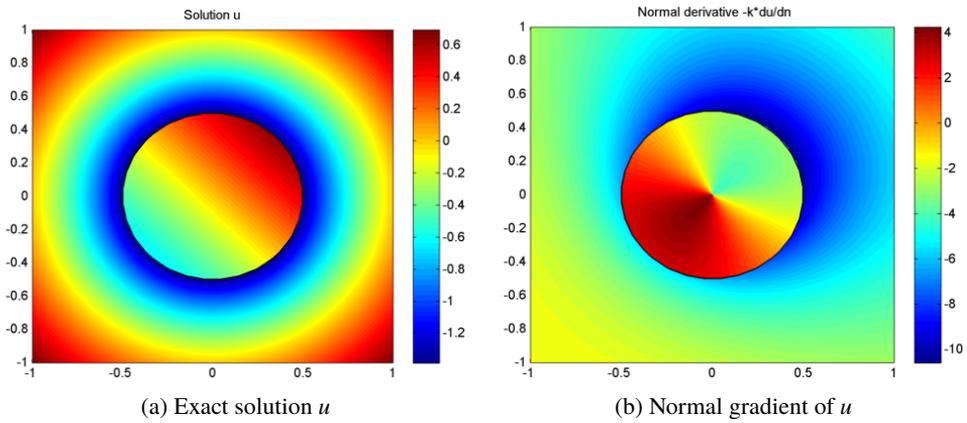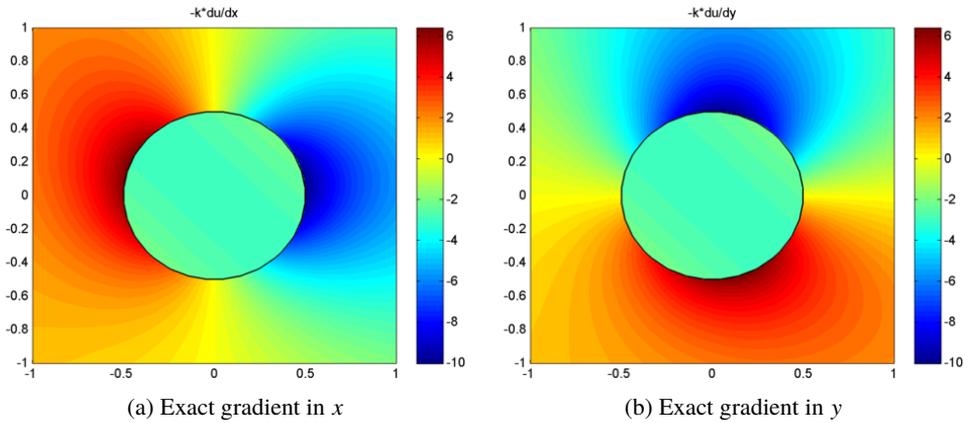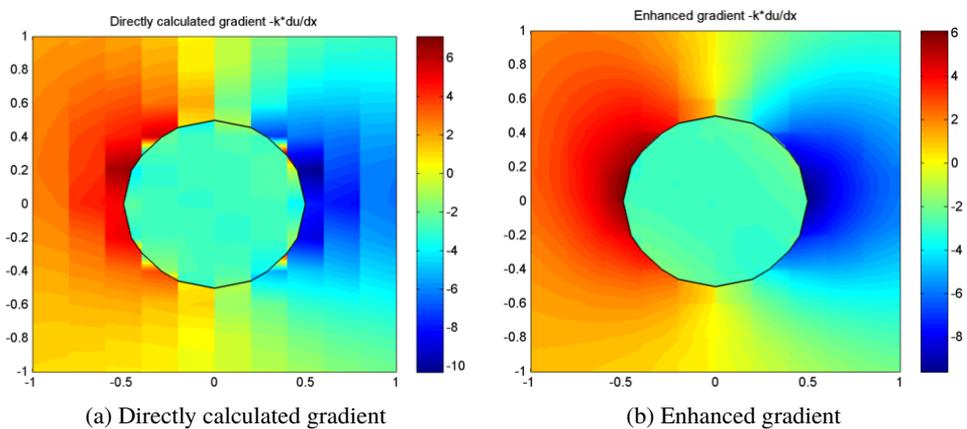
(a) Exact solution u

(b) Normal gradient of u

Fig. 6. 2D curved interface problem – exact solution and normal gradient

(a) Exact gradient in x

(b) Exact gradient in y

Fig. 7. 2D curved interface problem – exact gradient in x and y direction

(a) Directly calculated gradient

(b) Enhanced gradient

Fig. 8. 2D curved interface problem – calculated gradient in x direction

(a) Directly calculated gradient

(b) Enhanced gradient
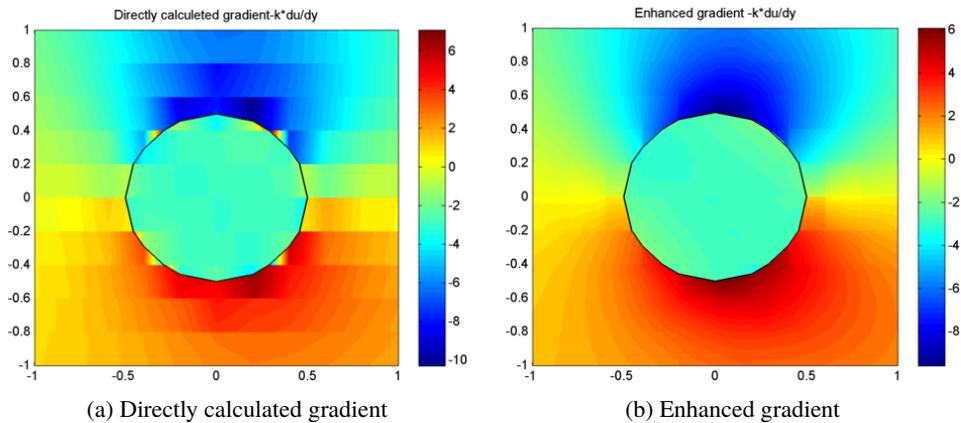
Fig. 9. 2D curved interface problem – calculated gradient in y direction

(a) L_2 and energy norm

(b) Condition number of the stiffness matrix
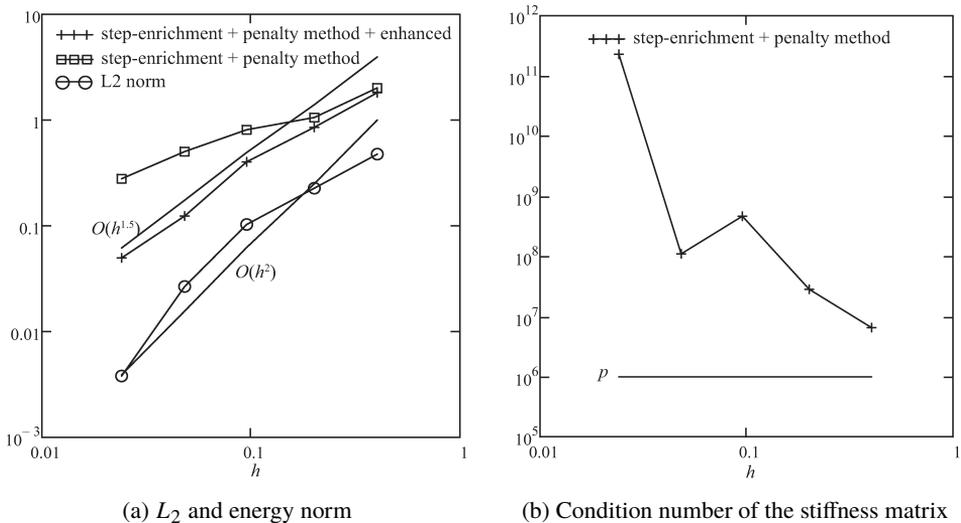
Fig. 10. 2D curved interface problem

8. Conclusions

In the paper, we presented the XFEM methodology for the efficient solution of 1D and 2D Poisson problems, in which the coefficients of equation as well as the solution and its gradient exhibit the jump across the internal interface. The standard approach was enhanced with the recovery procedure, which allows for better prediction of gradient with minimal computational cost. The convergence in energy norm is also improved. However, for 1D problems with both weak and strong discontinuities the $O(h^3)$ order is achieved, for 2D problems with straight interface the convergence also reaches $O(h^3)$ order, whereas for curved interface the order

declines to $O(h^{1.5})$. The reason for observed decline in the energy convergence order may be the approximation of the interface with linear shape functions, but it needs further research. The originality of the proposed method comes from the application of the recovery procedure to the elements with enriched approximation.

Acknowledgements

References

[1] P. Stąpór. An improved XFEM for the Poisson equation with discontinuous coefficients. *Archive of Mechanical Engineering*, 64(1):123–144, 2017. doi: 10.1515/meceng-2017-0008.

[2] T. Grätsch and K.-J. Bathe. A posteriori error estimation techniques in practical finite element analysis. *Computers & Structures*, 83(4-5):235–265, 2005. doi: 10.1016/j.compstruc.2004.08.011.

[3] M. Ainsworth and J.T. Oden. A posteriori error estimation in finite element analysis. *Computer Methods in Applied Mechanics and Engineering*, 142(1-2):1–88, 1997. doi: 10.1016/S0045-7825(96)01107-3.

[4] P.J. Payen and K.-J. Bathe. A stress improvement procedure. *Computers & Structures*, 112-113:311–326, 2012. doi: 10.1016/j.compstruc.2012.07.006.

[5] T. Belytschko and T. Black. Elastic crack growth in finite elements with minimal remeshing. *International Journal for Numerical Methods in Engineering*, 45(5):601–620, 1999. doi: 10.1002/(SICI)1097-0207(19990620)45:5<601::AID-NME598>3.0.CO;2-S.

[6] P. Stąpór. Application of XFEM with shifted-basis approximation to computation of stress intensity factors. *The Archive of Mechanical Engineering*, 58(4):447–483, 2011. doi: 10.2478/v10180-011-0028-0.

[7] D. Belsley, R.E. Welsch, and E. Kuh. *The Condition Number. Regression Diagnostics: Identifying Influential Data and Sources of Collinearity*. John Wiley & Sons, Inc., Hoboken, New Jersey, 1980.

[8] S. Hou and X.-D. Liu. A numerical method for solving variable coeffiecient elliptic equation with interfaces. *Jurnal of Computational Physics*, 202(2):411–445, 2005. doi: 10.1016/j.jcp.2004.07.016.